Central European Journal of Energetic Materials
ISSN 1733-7178; e-ISSN 2353-1843
Copyright © 2019 Łukasiewicz Research Network – Institute of Industrial Organic Chemistry, Poland

Cent. Eur. J. Energ. Mater. 2019, *16*(4): 596-606; DOI 10.22211/cejem/114056
Article is available in PDF-format, in colour, at:
http://www.wydawnictwa.ipo.waw.pl/cejem/Vol-16-Number-4-2019/CEJEM_01090.pdf
Article is available under the Creative Commons Attribution-Noncommercial-NoDerivs 3.0 license CC BY-NC-ND 3.0.

Research paper

X-ray and Visual Investigations on the Combustion Process of Curved, Low-gas, Pyrotechnic Paths Used in Self-destruction Assemblies of Missile Fusing Systems

Maciej Miszczak*, Radosław Warchoł, Marcin Nita

Military Institute of Armament Technology,
7 Prym. St. Wyszyńskiego street, 05-220 Zielonka, Poland
**E-mail:* mpf.miszczak@op.pl

Abstract: The validation of the consistency of combustion front propagation along confined, low-gas, curved, pyrotechnic paths pressed into the grooves of the disc bodies of artillery and rocket ammunition fusing systems, is of critical importance as it concerns the functional reliability and safe usage of such types of ammunition. To validate the above consistency, Real Time X-ray Radioscopy (RTR) was utilized for the recording of the combustion process of curved pyrotechnic paths comprising two delay time segments. To confirm the observations obtained by the RTR technique, visual (VIS) recording was utilized for the unconfined pyrotechnic path. Due to the RTR and VIS techniques, evolution of the combustion process was recorded as a combustion front travelling along the pyrotechnic path. The combustion front had a convex shape. Using the VIS technique, a conical, bright tail was also observed behind the combustion front. The mean velocity of the propagation of the combustion front along each delay segment of the confined pyrotechnic path was determined on the basis of the RTR recordings.
Using the RTR and VIS techniques, it was possible to quasi-continuously detect and record the combustion front movement along the confined and unconfined pyrotechnic paths, respectively. The VIS observations confirmed the RTR recording of the convex shape of the combustion front. In addition, the VIS technique allowed us to record the bright, conical tail.

Keywords: combustion, military ammunition, pyrotechnic curved paths, optical recording

1 Introduction

The application of pyrotechnic paths pressed into ring grooves of time delay fuses of artillery shells and rockets have a history of over a century [1-24]. With the development of such types of fuses, black powder [1-9] was gradually replaced by pyrotechnic compositions of slower burning rate and/or liberating smaller amounts of gaseous combustion products [10-24]. Interesting test results on the dependence of the burning rate of modern, low-gas, pyrotechnic, ring shaped paths on their initial temperatures, are presented in [22-24].

Not exactly ring shaped, low-gas pyrotechnic paths, but ones with circular shapes are used in self-destroying timing assemblies of short-range, anti-aircraft missiles in service with the Polish Army. In order to obtain more detail about the evolution of the combustion process in such paths, confined (covered) ones were selected for the recording of their burning process by means of Real Time X-ray Radioscopy (RTR), together with unconfined (uncovered) ones for recording of their burning by a visual (VIS) camera.

2 Test Samples

The self-destroying timing assemblies were extracted from anti-aircraft short range missiles. Each assembly comprised a plastic body with a cylindrical cavity housing the input and output ignition channels. The output ignition channel communicated with the detonation cap of the warhead high explosive charge. This body also accommodated a steel disc housing a pressed, curved, segmented delay timing pyrotechnic path covered by a sealing felt disc which separated the pyrotechnic path from the bottom of the plastic body cavity. Both discs and the bottom surface of the plastic body cavity were secured tightly in place and had a diameter of 25.8 mm. The steel disc was 4.2 mm thick. The pyrotechnic path (Figure 1) was *ca.* 55.7 mm long, 3 mm wide and 3 mm deep.

Copyright © 2019 Łukasiewicz Research Network – Institute of Industrial Organic Chemistry, Poland

Figure 1. Unconfined (uncovered), curved, segmented pyrotechnic path pressed into the groove of the steel disc of a self-destroying timing assembly of an anti-aircraft short range missile

The first ignited pyrotechnic segment, *i.e.* the input ignition one, is the first one from the right of the pyrotechnic path (Figure 1). The next two ignited segments of the pyrotechnic path, the short and long delays, are responsible for the generation of a substantial part of the delay period of the self-destroying timing assembly. The final ignited pyrotechnic segment of the pyrotechnic path, is the output ignition one.

The input and output ignition segments were composed of 74.5% lead(II, IV) oxide (Pb_3O_4), 23.5% zirconium powder and 2% collodion nitrocellulose. This pyrotechnic composition burns vigorously with a relatively high rate even at low pressure. The short delay segment, *ca.* 6 mm long, was composed of 81% barium chromate(VI) ($BaCrO_4$), 9% potassium chlorate(VII) ($KClO_4$), 8% sulfur, and 2% collodion nitrocellulose. The long delay segment, *ca.* 46 mm long, was composed of 77.5% $BaCrO_4$, 10.5% antimony pentasulfide (Sb_2S_5), 10% $KClO_4$ and 2% collodion nitrocellulose.

3 Test Methods

Each investigated self-destroying timing assembly (containing a covered pyrotechnic path) was inserted into the detection chamber of a Real-Time X-ray Radioscopy (RTR) MU-17F-225-9 diagnostic system (YXLON International X-ray Corporation), and then examined for defects by X-rays (Figure 2).

Copyright © 2019 Łukasiewicz Research Network – Institute of Industrial Organic Chemistry, Poland

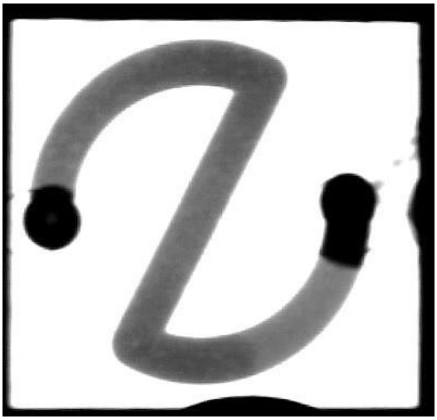

Figure 2. RTR image of a confined (covered) curved, segmented pyrotechnic path of a self-destroying timing assembly of an anti-aircraft short range missile

Figure 2 shows that the pyrotechnic path had no distinct structural defects, such as voids and/or cracks. The input and output ignition segments are the darkest ones due to the presence of lead in their compositions.

After X-ray examination, each test sample was ignited in the RTR chamber by an electric fuse-head. Combustion of the covered pyrotechnic path was detected and recorded by the RTR diagnostic system, at 30 fps and a resolution of 1528 × 1052 px.

Each investigated uncovered (open) disc with the pyrotechnic path, was also visually examined using a VIS camera (Figure 1). Figure 1 confirms (as in the case of RTR examination) that the pyrotechnic path of the self-destroying timing assembly had no distinct structural defects, such as voids and/or cracks. After VIS examination, each test sample was ignited by an electric fuse-head. Combustion of the uncovered pyrotechnic path was detected and recorded by the VIS camera at 50 fps and a resolution of 1920 × 1080 px.

4 Results and Discussion

4.1 RTR recordings

A typical sequence of RTR images (frames) selected from the RTR film, is shown in Figures 3(a) to 3(r), successively presenting the ignition and fast burning of the input ignition pyrotechnic segment (Figures 3(a) and 3(b)), burning of the short delay segment (Figures 3(c) to 3(f)), burning of the long

Copyright © 2019 Łukasiewicz Research Network – Institute of Industrial Organic Chemistry, Poland

delay segment (Figures 3(g) to 3(p)), and finally ignition and fast burning of the output ignition pyrotechnic segment (Figures 3(q) and 3(r)).

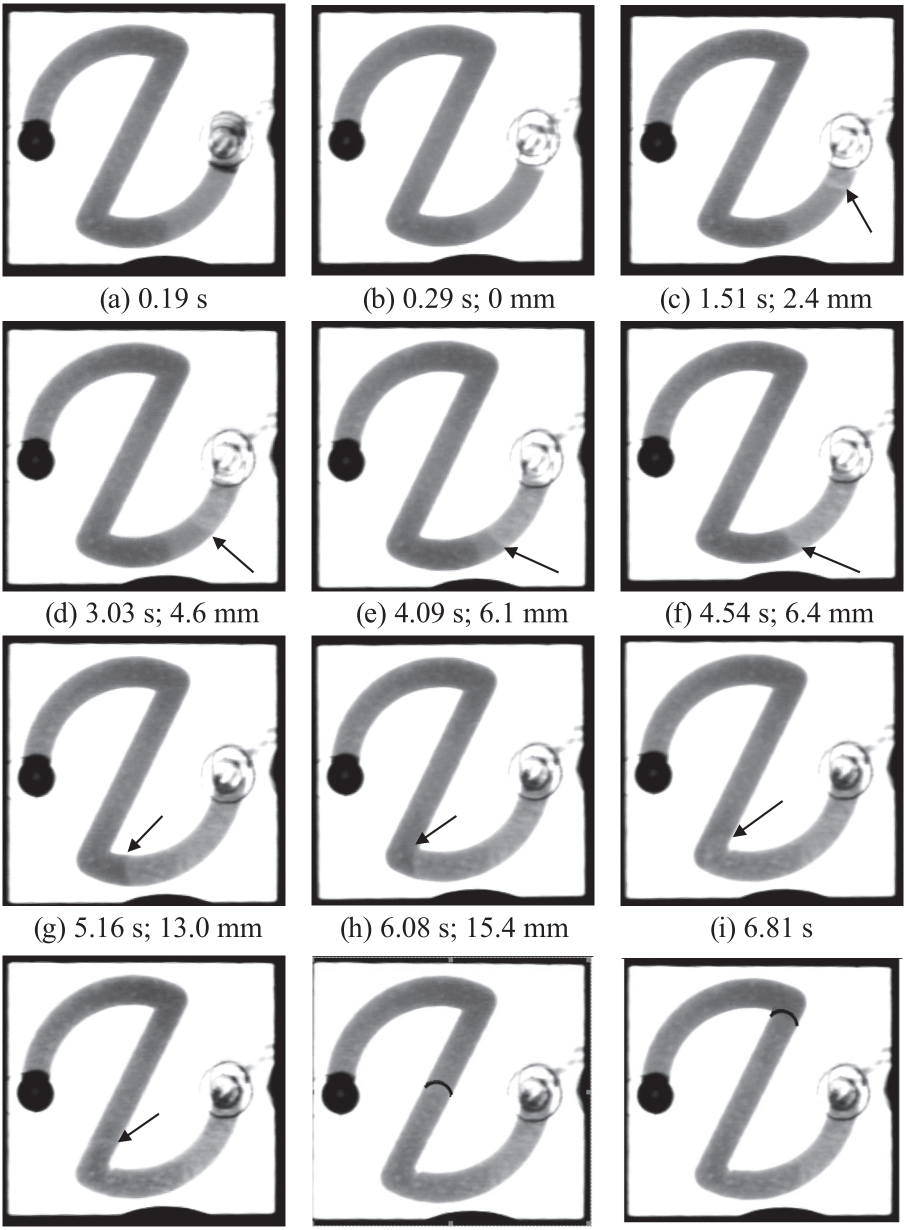

(a) 0.19 s (b) 0.29 s; 0 mm (c) 1.51 s; 2.4 mm

(d) 3.03 s; 4.6 mm (e) 4.09 s; 6.1 mm (f) 4.54 s; 6.4 mm

(g) 5.16 s; 13.0 mm (h) 6.08 s; 15.4 mm (i) 6.81 s

(j) 7.33 s; 20.9 mm (k) 8.96 s; 25.7 mm (l) 11.89 s; 33.3 mm

Copyright © 2019 Łukasiewicz Research Network – Institute of Industrial Organic Chemistry, Poland

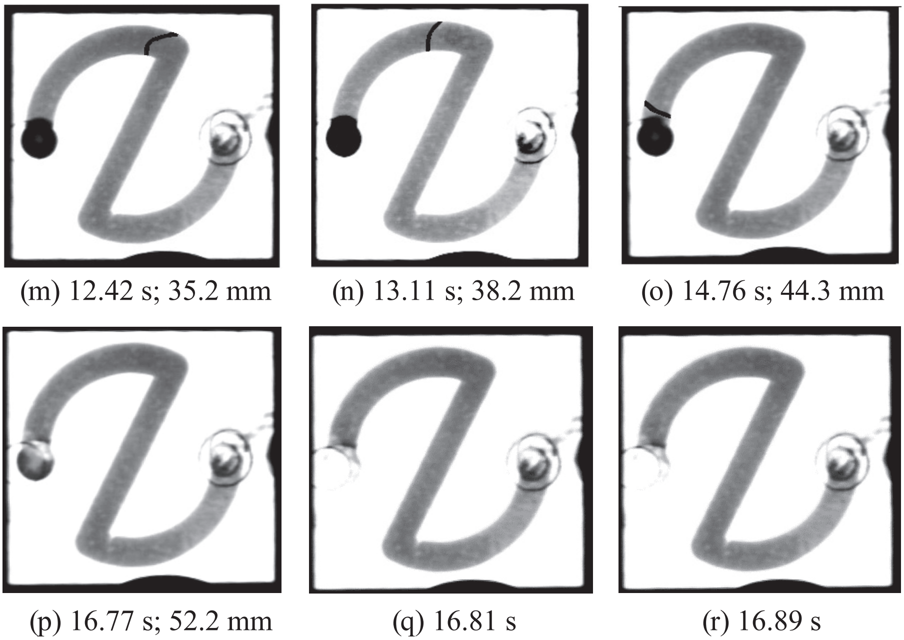

Figure 3. Sequence of RTR images showing the combustion of a confined, curved, segmented pyrotechnic path of the self-destroying timing assembly of the fusing system of an anti-aircraft short range missile *Note: In Figures 3(c) to 3(j), the positions of the combustion front are indicated by arrows, but for Figures 3(k) to 3(p), the combustion front positions are* indicated as *black arcs.*

It was possible to observe the evolution of the combustion process as the combustion front travelled along all of the pyrotechnic segments of the pyrotechnic path. The combustion front was visualized as a moving convex border between the burnt and unburnt parts of the pyrotechnic path. The length of the combustion front, *i.e.* its length between the opposite side walls of the pyrotechnic path, varied during the course of the combustion process. The longest combustion front occurred at the turnings of the pyrotechnic path (Figure 3(i)).

On the basis of the RTR images, it was possible to determine important parameters of the self-destroying timing assembly as concerns its reliable functioning and safe usage in the missile fusing system. These parameters were: the total burning time of the confined pyrotechnic path and its mean burning rate. The total burning time of the pyrotechnic path should last between 14 and 17.5 s, counted from the firing of the missile to its destruction during flight if the missile misses the air-target.

Copyright © 2019 Łukasiewicz Research Network – Institute of Industrial Organic Chemistry, Poland

From the RTR frame which registered the first symptoms of ignition of the input pyrotechnic segment (Figure 3(a)) to the frame which registered the opening of the channel accommodating the output ignition segment due to its partial burn out (Figure 3(q)), it was estimated that the total burning time of the tested self-destroying timing assembly was *ca.* 16.8 s.

The total length of the pyrotechnic path measured along its central line (including input and output ignition segments), was *ca.* 55.7 mm, so the mean burning rate of the whole pyrotechnic path was estimated as *ca.* 3.3 mm/s.

In order to obtain more detailed data on the dynamics of the burning process in its most decisive stages for the delay time, the mean burning rates of the short and the long delay pyrotechnic segments were determined. The time coordinates of the combustion front travelling along these segments were determined as the time points of the RTR frame recordings. The position coordinates of the combustion front, corresponding to the time coordinates, were obtained as a result of the intersection of the central line of the pyrotechnic path with the combustion front. On the basis of selected RTR frames (Figures 3(b) to 3(e), Figure 3(g), Figure 3(h), Figure 3(j), and Figures 3(k) to 3(p)), a plot of the combustion front positions *versus* their time coordinates was created (Figure 4).

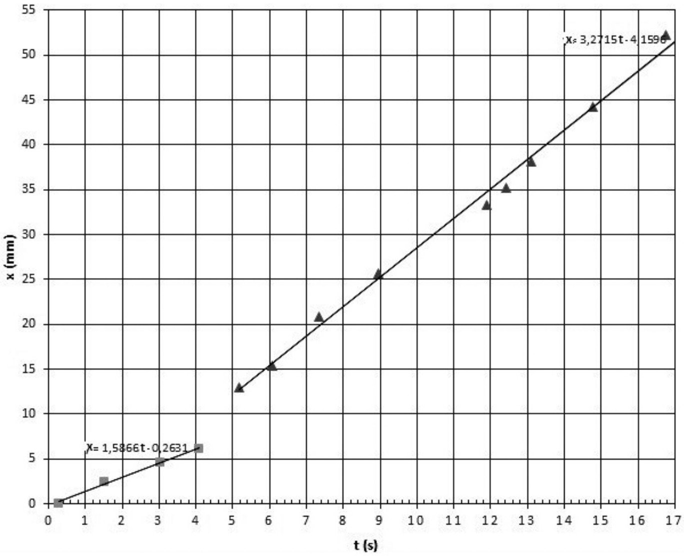

Figure 4. Plot of combustion front position coordinates (x) *vs.* time (t) points corresponding to these position coordinates for short and long delay segments of the confined pyrotechnic path, (registered by the RTR technique), and regression straight lines obtained for the short and long delay segments, respectively

Copyright © 2019 Łukasiewicz Research Network – Institute of Industrial Organic Chemistry, Poland

The combustion front positions shown in Figures 3(f) and 3(i), were not taken into consideration in the creation of the distance-time plot (Figure 4) because in Figure 3(f) the combustion front seems to intersect the border line between the short and long delay segments, and in Figure 3(i) the combustion front position is difficult to determined precisely in relation to the central line of the pyrotechnic path.

On the basis of the value obtained for the direction coefficient (slope) of the first regression line attributed to the short delay pyrotechnic segment (Figure 4), its mean burning rate was estimated as 1.6 mm/s. On the basis of the value obtained for the direction coefficient (slope) of the second regression line attributed to the long delay pyrotechnic segment (Figure 4), its mean burning rate was estimated as 3.3 mm/s.

4.2 VIS recordings

A typical sequence of VIS images (frames) selected from the video-camera film, is shown in Figures 5(a) to 5(j), presenting burning of the uncovered short (Figures 5(a) to 5(d)) and long delay segments (Figures 5(e) to 5(j)), respectively.

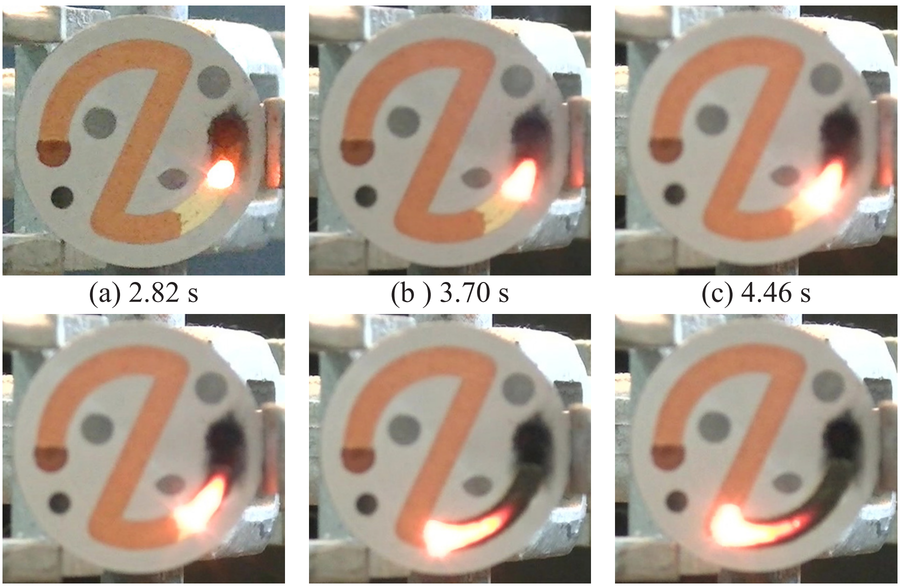

(a) 2.82 s (b) 3.70 s (c) 4.46 s

(d) 5.26 s (e) 7.88 s (f) 8.68 s

Copyright © 2019 Łukasiewicz Research Network – Institute of Industrial Organic Chemistry, Poland

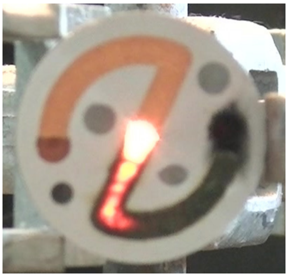
(g) 11.38 s

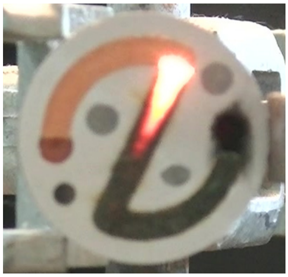
(h) 14.02 s

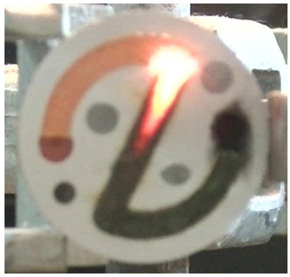
(i) 14.22 s

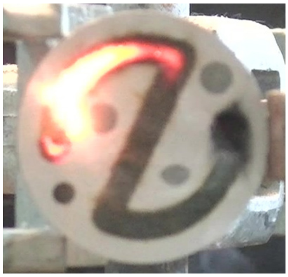
(j) 18.02 s

Figure 5. Sequence of VIS images showing the combustion process of an uncovered (unconfined), curved, low-gas, segmented pyrotechnic path

The development of the combustion process could be observed as the combustion front and, adjacent to it the bright, long, conical tail stretching behind it, both travelling along the short and long delay pyrotechnic segments. The combustion front was visualized as the moving convex border between the burnt and unburnt parts of the pyrotechnic path. The length of the combustion front, *i.e.* its length between the opposite side walls of the pyrotechnic path, varied during the course of the combustion process. The longest combustion fronts occurred at the turnings of the pyrotechnic path, *i.e.* at sections connecting its curved parts with the straight part (Figures 5(f) and 5(i)). The length of the tail varied in the course of the combustion process. The total burning time of the uncovered pyrotechnic path was longer than 18 s. In Figures 5(b) to 5(j) the uncovered pyrotechnic path is screened to some extent by its gaseous combustion products not evolving intensely.

Copyright © 2019 Łukasiewicz Research Network – Institute of Industrial Organic Chemistry, Poland

5. Summary and Conclusions

Using the RTR technique, it was possible to quasi-continuously detect and record the combustion front movement during the burning of the confined (covered) curved, low-gas, segmented, pyrotechnic path in the self-destroying timing assembly of an anti-aircraft short range missile fusing system.

The VIS recording of the combustion process of the unconfined (uncovered) curved, low-gas pyrotechnic path, confirmed not only the RTR observations on the combustion front shape and its evolution during burning of the confined pyrotechnic path, but they allowed us to obtain information on the occurrence of the bright, conical, long tail extending behind the combustion front and adjacent to it. It seems that the conical shape of this tail was caused by gradual cooling of the condensed (mainly solid) combustion products which started to cool from the periphery (side) layers of the pyrotechnic path towards its center line.

The combustion front movement along the short and long delay segments of the confined pyrotechnic path, was stable because this front travelled along each segment with an estimated constant velocity. The total delay time of the confined pyrotechnic path used in the self-destroying timing assembly of the fusing system of the anti-aircraft short range missile, was consistent with the requirements concerning the total delay time for this type of military munition.

The burning time of the unconfined pyrotechnic path was distinctly longer than the burning time of the same type of pyrotechnic path confined in the body of the self-destroying timing assembly. This difference in burning times was probably caused by the pressure build-up from the gaseous products liberated during the combustion of the confined pyrotechnic path.

References

[1] *Encyclopedia of Explosives and Related Items*. Vol. 4, (Fedoroff, B.T.; Sheffield, O.E., Eds.), Picatinny Arsenal, Dover, NJ, **1969**, pp. D.857-858, D.860, D.862.

[2] Hathaway, G.M.; Hathaway, C.F. *Fuse for Shells.* Patent US 729932, **1903**.

[3] King's Norton Metal Co. and others, *Improvements in Fuses for Shells and other Explosive Projectiles.* Patent GB 5654, **1909**.

[4] Rheinishe Metalwaaren-und Mashinen Fabrik, *An Improved Percussion Fuse for Projectiles in Which, if Desired, the Explosion Can Be Delayed by a Certain Amount after Percussion*. Patent GB 18890, **1912**.

[5] Carr, M.F. *An Improved Time Fuse for Projectiles.* Patent GB 108429, **1917**.

[6] Austin, H. *Improvements in Time Fuses for Explosive Shells and Bombs.*

Copyright © 2019 Łukasiewicz Research Network – Institute of Industrial Organic Chemistry, Poland

Patent GB 124806, **1919**.
[7] Goss, J.H. *Fuse for Projectiles.* Patent US 1508450, **1924**.
[8] Pantoflicek, B. *Pyrotechnic Safety Device, i.e. Combustible One.* (in Polish) Patent PL 6215, **1927**.
[9] Vickers Co. Ltd. and Johnson, F.G.L. *Improvements in or Relating to Time Fuses for Projectiles.* Patent GB 282120, **1927**.
[10] Curtis's and Harvey Ltd. and Grimwood, A.J., *Improvements in and Relating to Fuse Compositions and to Fuses for Shells.* Patent GB 283741, **1928**.
[11] Hale, G.C. *Delay Powder.* Patent US 1805214, **1931**.
[12] Hale, G.C. *Delay Powder*. Patent US 1877127, **1932**.
[13] Hercules Powder Company, *Improvements in Fuses for Explosive Shells.* Patent GB 384776, **1932**.
[14] Imperial Chemical Industries Co. Ltd., *Improvements in or Relating to Fuses and Like Combustion Train Elements.* Patent GB 492438, **1938**.
[15] Hale, G.C. *Delay Powder.* Patent US 2450892, **1948**.
[16] Hale, G.C.; Hart, D. *Delay Powder.* Patent US 2478918, **1949**.
[17] Nowak, K. *Disc Shaped Pyrotechnic Delay Element.* (in Polish) Patent PL 72424, **1975**.
[18] Simmons, B.H.O. *Pyrotechnic Delay Devices.* Patent US 1434788, **1976**.
[19] Kaczmarski, S.; Kuśnierz, T.; Zarzycki, B. *Artillery Fuse with Adjustable Delay Element*. (in Polish) Patent PL 144528, **1988**.
[20] Shevchenko, A.M.; Serdjukova, V.N.; Syzrantzev, V.F. *Safety-Actuating Mechanism for Warheads of Rocket Ammunition.* (in Russian) Patent RU 2301960, **2007**.
[21] Gao, Z.; Yuan, L.; Cheng, K.; Li, G.; Li, C. *Fuse Powder Ring Device for Artificial Hail Preventing and Precipitation Increasing Projectile.* Patent CN 105890472, **2016**.
[22] Khurmatulina, R.I.; Minibaeva, D.G.; Smetanina, N.D.; Maltseva, T.G.; Petrova, V.A.; Golubev, V.S. *Low-Gas Slow Burning Compound.* (in Russian) Patent RU 2185355, **2002**.
[23] Ardasheva, L.F.; Minibaeva, D.G.; Smetanina, N.D. *Retarding Low-Gas Compositions.* (in Russian) Patent RU 2256638, **2005**.
[24] Okhrimenko, Eh.F.; Minibaeva, D.G.; Smetanina, N.D. *Retarding Low-Gas Composition.* (in Russian) Patent RU 2237646, **2004**.

Received: August 2, 2019
Revised: November 6, 2019
First published online: December 20, 2019

Copyright © 2019 Łukasiewicz Research Network – Institute of Industrial Organic Chemistry, Poland